

## Large scale concrete cube blasts for the HSBM model

E.J. Sellers & M. Kotze

*African Explosives Limited, South Africa*

L. Dipenaar

*Anglo-American, South Africa*

M. Ruest

*De Beers, South Africa*

**ABSTRACT:** Four, large scale, calibration test blasts have been done for the HSBM project by constructing concrete cubes of 3 m side length to provide a uniform material for comparison with model results. The amount of explosive (600 g) and borehole diameter (33 mm) were selected to reproduce realistic non-ideal detonation response in the explosive column and cause significant fracturing, but not total destruction, so that the situation is suitable for comparison with the numerical model. The design philosophy and experiences from performing these tests are presented in this paper. The blasts were monitored using high speed cameras, velocity of detonation probes, geophones and accelerometers. Two cubes experienced significant heave and fragmentation whereas the other two broke into large segments that were only displaced slightly. Thus, it appears that the selected burden of 0.8 m is just on critical and this provides another constraint on the modelling. Limited model comparisons indicate that the modeled peak particle velocities from the model are at the lower end of the measured results. Waveform shapes are similar, but are dependent on the wave speed due to the superposition of reflections from the side of the cube. Modelled waveforms indicate that the period of the waveform increases with charge size and decreases with VoD. The amplitude decreases with charge size and increases with VoD. Hopefully, both the test data and the learning from performing these experiments will be of use to the broader blasting community in future.

### 1 INTRODUCTION

The Hybrid Stress Blasting Model (Furtney et al. 2009) is an international collaboration project to develop a numerical model that can represent the mechanics of the rock blasting process, from detonation through fracturing and heave to predict the ultimate muck pile profile. The first implementation of the model used particle methods (Ruest et al. 2006, Potyondy & Cundall 2004) to represent the rock mass and permit gas flow and fragment interactions subsequent to the blast. However a lattice representation of the rock mass and a simplified gas model have been implemented in the latest version to improve memory usage and run times (Furtney et al. 2009). A programmed burn model (Cundall & Detournay 2008) links with detonation codes (Cunningham et al. 2006, Braithwaite et al. 2009) to determine the shock front pressure and subsequent detonation characteristics.

Any numerical model requires calibration and validation. This is extremely difficult in the blasting environment due to the high pressures, velocities

and temperatures that require specialized sensors, the shock conditions and fracturing which tend to destroy the sensors and the rapidity of the processes that require high data acquisition rates and produce huge quantities of data. As with any geomaterial modelling, the variation in the structure of the rock mass creates difficulties in comparing similar situations. A literature study was undertaken to find suitable experiments to model. It is important to have sufficient information from a test to be able to conclusively compare model results and to be able to distinguish the effects of the explosive and materials. At least 42 papers were found of which about 10 had sufficient information to permit modelling with minimal assumptions. Suitable tests for modeling range from the small scale of 25 cm to 50 cm blocks (Dick et al. 1993, Katsabanis et al. 2006) using PETN as explosive; through smaller scale field tests with emulsions and dynamites at scales of 50 cm (Kristiansen et al. 1990), 1 m (Esen et al. 2003) and 2 m (Bergmann et al. 1973); to large scale field tests (e.g. Ouchterlony et al. 1996, Stagg & Rhol 1987). Because the accurate representation of

the non ideal performance of commercial explosives has been a focus of the HSBM detonation research, it is vital that any validation testing is done at a scale that is representative of field performance of these products. However, most of the smaller scale modelling efforts have either used ideal explosives such as PETN or very small amounts of emulsion or dynamite where it is unclear if the product has performed optimally. On the other hand, field scale tests include the effect of geological disturbances and, due to the fine discretization required for the numerical models, generally require computational turnaround times that are too long for a calibration exercise. Thus, it was realized that is important to perform tests using a significant amount of non ideal explosive and having velocity and acceleration measurements within the solid surrounding the blast hole. It was therefore decided to perform a series of experiments in concrete at a relatively large scale.

To date, four large scale calibration test blasts have been done for the HSBM project by constructing concrete cubes of 3 m side length to provide a uniform material for comparison with model results. The amount of explosive (600 g) and borehole diameter (33 mm) were selected to reproduce realistic non-ideal detonation response in the explosive column, cause significant fracturing, but not total destruction so that the situation is suitable for comparison with the numerical models. The tests have been very successful. This paper presents a discussion of the experiments and the learning associated with this process. The velocities and accelerations measured in the cubes, the resultant fracturing and fragmentation, and the face velocities recorded by high speed camera are discussed in the context of preliminary numerical modelling results.

## 2 CONSTRUCTION

The cubes were cast in a disused sand quarry near Bronkhorstspuit, about 1 hour drive North East of Johannesburg, South Africa. Initially, the plan was to cast the cube on the floor of the current pit. However due to excessive rains this was not possible. The first cube was cast on a flat area on a higher level, just at the end of the entrance ramp. Unfortunately there was a pit wall about 2 m from one side of the cube and a slope at the back of the cube. The next three cubes were cast on a wide causeway that has been built through the water in the bottom of the pit.

Each site was initially leveled and a grid of steel reinforcing rods in plastic pipes was placed on the surface to act as cross ties for the bottom part of the shuttering. A small covering of sand was then placed over the grid to provide a level base for

the cube. Shuttering was erected for the 3 m by 3 m by 3 m cube (Figure 1). A grid of reinforcing steel in plastic pipes was placed on top and connected through the top beams by plates welded on the outside. This allowed for a small amount of slack that was only taken up once the concrete was being poured. The first cube was cast successfully, but the shuttering deformed creating a slight barrel shape. The shuttering system of uprights and angled braces was insufficient to restrain the shuttering and so a set of four I-beams were placed halfway up the cube, tightened against the formwork and welded to form a closed loop in order to constrain the movement and prevent buckling of the vertical struts.

The first cube was cast on the 21 April 2008 using concrete of nominal 40 MPa strength with 19 mm aggregate. Concrete pouring started at about 9 am and was completed at 7.30 pm. The outside temperature was about 10°C and the temperature went down to 0°C overnight. The cube had not set properly the next day when the team returned to strip the shuttering. Shuttering was eventually stripped about a week later. The concrete appeared to be slightly damp at the core of the cube after the blast was performed a month later.

The next three cubes were cast during August and September 2008. The second block had to be cast over two days due to construction delays resulting in a construction joint about 0.7 m from the top (Figure 2). There does not seem to have been any significant effect of the joint on the final fracture pattern. Chemical accelerators were used to decrease setting times in the third and fourth block and significantly improved the shape of the cubes.

The blast hole was created by driving a 33 mm diameter steel rod into the wet concrete. The rod was oiled slightly to assist with removal. The rod had a block welded to the exposed end and between



Figure 1. Shuttering for cube.



Figure 2. Second cube as cast.

this block and the concrete there was a 100 mm diameter steel cylinder surrounding the rod to act as a hammer to lift the rod once the concrete was dried. Two planks were placed on either side of the rod to support the hammer cylinder while the concrete dried. In all cases, however, the rod could only be extracted using two ten ton jacks.

Strength tests were done on cylinders drilled from the cube samples made at the concrete plant. The concrete has an average strength of 45 MPa, the Young's modulus ranges from 23 GPa to 37 GPa, and Poisson's ratios were from 0.1 to 0.23. Tensile strengths varied from 2.9 to 6.5 MPa. Sonic wave velocities on the concrete were measured in the laboratory to be  $3316 \pm 1120$  m/s and calculations from the measured elastic properties gives  $4014 \pm 455$  m/s.

### 3 INSTRUMENTATION

In the first block the geophones and accelerometers were glued onto H shaped aluminium rods and cast at depths ranging from 0.9 to 1.0 m below the top surface, at distances of 0.5, 1.0 and 1.5 m directly behind the borehole. The uniaxial geophones can record a maximum velocity of 0.95 m/s, which is very low relative to the expected velocities. The accelerometers are rated for 2000 g with a shock limit of 5000 g.

The geophones and 2000 g accelerometer all saturated in the first cube and so 100 000 g accelerometers were purchased. For subsequent tests, the geophones and 2000 g accelerometers were moved to a position 300 mm from the top back corner of the cube which received some vibration, but were displaced significantly and did not saturate. Three geophones were placed orthogonally on a 5 mm diameter aluminium rod that was bent to create a 3D array. The three geophones were aligned parallel

to the sides (x direction), parallel to the back face (y direction) and vertically (z direction).

The H-shaped aluminium rods used in the first block caused debate about what would be the effect of waves travelling up the rod on the measurements so the PCB accelerometers were each cast into a separate concrete rod of triangular cross section to attempt to remove any modulus contrast in the cube. The rods were cast off site using 75 mm angles as shuttering, so that the short sides were 50 mm long. It proved to be easy to push the rods into the concrete once the shuttering was filled and the mass concrete was then vibrated around the rod. Examples of the cast rods are shown in Figure 3. Even though a single wire was cast along the length of the rod, cracking appeared during transport to site due to the low tensile strength of the concrete. A plan view layout of all the instruments is shown schematically in Figure 4 and an elevation view is shown in Figure 5.

The problems of casting the rods off site and cracking, as well as limited time available meant that a different system was used for the fourth cube. In this cube, the accelerometers were fixed to perforated aluminium angles. The sensors were case into about 80 mm of concrete using a paper cup as a mould. These rods were then placed into the wet concrete.

A 12 channel TLC Transcap device was used to log the accelerometers and geophones. The device uses 12 bit technology and logs at 5 Mhz and was modified to allow of independent voltages on each set of 4 channels so that the sensitivity could be optimized for the various devices.

Two resistance probes were placed in each borehole to measure the velocity of detonation (VoD), one connected to the Transcap and the other to a MREL logger. A resistance probe was cast into the concrete next to the borehole as a backup.



Figure 3. Top view of a cube showing triangular concrete rods. White circle indicates the borehole.

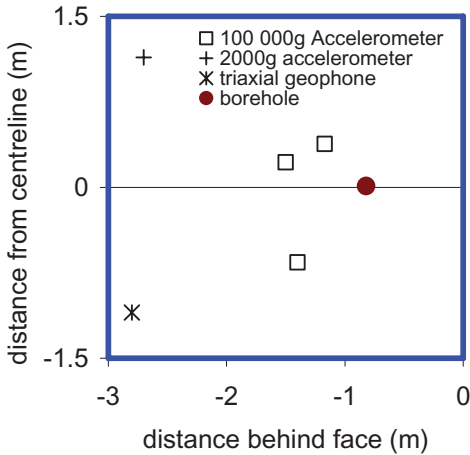


Figure 4. Schematic plan of instrumentation.

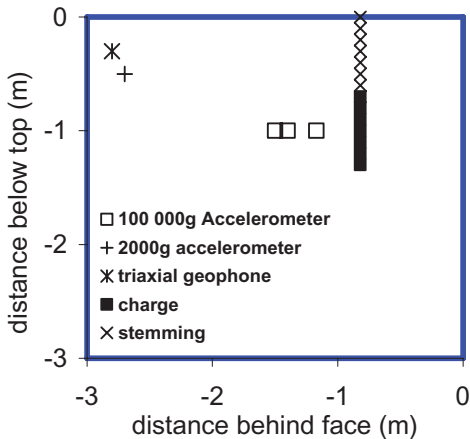


Figure 5. Schematic side view of instrumentation.

For each blast, there were up to 4 high speed cameras (1000 fps). These cameras were aligned to take side on shots for velocity tracking as well as angled shots for monitoring the fracturing. The frame rate is insufficient to monitor the fracture processes within the block. Each cube was painted in a 0.5 m grid of 75 mm to 100 mm wide strips on the day before the blast. This provides contrast to distinguish the cubes from their surroundings and proved to be invaluable for evaluating the throw trajectories from the video.

#### 4 BLAST DESIGN PHILOSOPHY

The design philosophy of the experiment was to break the blocks in a manner that would be most useful for numerical modeling. The aim was to

leave a portion of the cube intact as it would be difficult to model if the entire cube was shattered. The design aimed to simulate a surface bench as much as possible. The hole was required to lie in the top half of the block to limit the effects of the base. From the rules of thumb of blast design (Bergmann et al. 1973, AEL 2000), the charge should be greater than half the borehole length, the burden should be 24 to 36 times the diameter, the stemming 20 to 40 times the diameter, and the borehole length at least 50 times the diameter. Not all these parameters could be met, but led to the final design of a 33 mm borehole with 800 mm of burden and 606 g of explosive at a density of 1.18 g/cm<sup>3</sup>. The charge length is thus 600 mm long and the 1.3 m long borehole contains 700 mm of stemming. This also led to an overall powder factor of 0.02 kg/m<sup>3</sup>, which is lower than required for secondary breaking and hence the fragmentation would be expected to be controlled by the interaction of the borehole and the burden and not due to splitting of the cube.

Much debate ensued around whether to vary any of the blast design parameters between cubes. It was decided to keep all the design parameters constant for this set of cubes to evaluate the variations that are to be expected in an experimental set up of this scale.

#### 5 EXPLOSIVES AND CHARGING

The explosive selected was the SDS<sup>TM</sup> formulation from AEL. This is a small diameter emulsion explosive containing about 75% ammonium nitrate. The heat of reaction is 3.0 MJ/kg and the ideal velocity of detonation is calculated to be 6.2 km/s using the Vixen2009 code (Braithwaite et al. 2009). A VoD of 4500 m/s was measured in a 25 mm cardboard pipe. The formulation is usually sensitized underground using a dual phase gassing solution, but for this experiment it was decided to sensitize using microballoons so that the density could be obtained exactly. A density of 1.18 g/cm<sup>3</sup> was selected to provide optimum energy for the small diameter (33 mm) and length of charge (0.6 m) selected.

The hole was dewatered before charging. Charging proved to be problematic as the microballoon emulsion was very viscous and did not flow. The aim of the experiment was to be able to ensure that the explosive was fully coupled, but the difficulties of placing the product and ensuring the correct mass of explosive per hole meant for the third and fourth cubes, the emulsion was placed into thin plastic tubes. Two tubes were used for each cube. The tubes were slit completely, slid down and tamped individually. The tamping was continued until full coupling was achieved. Obviously, this left the plastic tube in an unknown position in the hole.

The hole was stemmed with coarse, uniform, sieved sand from the quarry crusher with a grain size of about 3 mm. This resulted in a grain size to diameter ratio of 11, which is acceptable (AEL 2000). A bag of sand was placed on top of the borehole for additional confinement and to contain the detonator for safety during charging.

For safety reasons, including the possibility of lightning, the need to recover misfires, shocktube detonators were used. A shocktube detonator with a 4 second delay was placed down the hole in a reverse primed configuration. The shock tube was initiated on the surface of the cube using an electric detonator connected to a shot exploder. A cable was tied to the down hole detonator so that a cut would trigger the logging system. The data showed that the triggering only happened well after the blast initiated. This is possibly due to the confinement of the small hole, or the conductivity of the explosive and so on the fourth cube, the cable was tied to a separate detonator on surface. This triggered about 20 ms before the main blast.

A risk assessment was conducted on the site and the procedures prior to the blast date. Appropriate safety measures were put in place. The height of the blocks and limited working space means that instrumentation connection and charging processes must be done carefully. At the start of the experiments there was no experience to determine maximum distances of throw so people manning the cameras and observing the blast were placed at least 100 m away. Only unmanned standard video cameras were placed in line with the expected breakout.

## 6 BLAST RESULTS

The fracture pattern surrounding the borehole in the first cube is shown in Figure 6. This is typical of the fracture patterns and shows radial cracks and damage. Snapshots from the high speed



Figure 6. Final fracture pattern of cube 1 looking directly over borehole.

cameras are shown in Figure 7 for the four blocks. The corresponding displacement—distance plots are shown in Figure 8. A summary of the results is given in Table 1.



Figure 7. Photographs captured from high speed videos for cubes 1, 2, 3 and 4 (top to bottom) respectively.

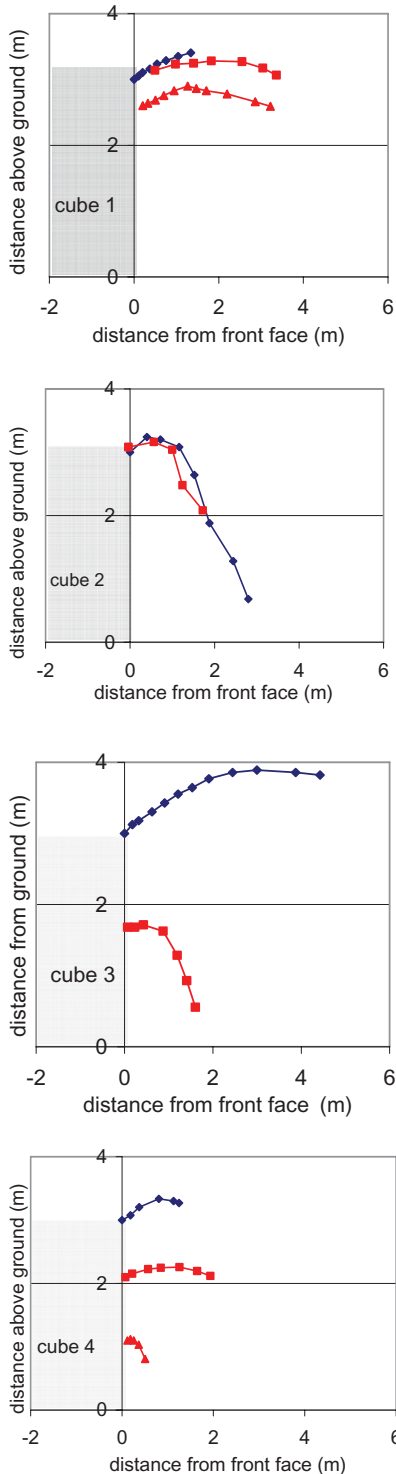


Figure 8. Throw trajectories calculated from high speed videos for cubes 1, 2, 3, 4.

Table 1. Summary of test results.

Cube	VoD (m/s)	VoD distance (m)	PPV at geophone (m/s)	Throw velocity (m/s)
1	none	n/a	n/a	8.6
2	3033	0.45	0.362	3.4
3	4397	0.5	1.189	8.4
4	none	n/a	0.893	3.4

In the first blast, the burden was ejected upwards and outwards. The region directly in front of the borehole was well fragmented. The large piece breaking off the side of the cube in the upper photograph of Figure 7 landed intact whereas the equivalent large piece on the far side side hit the quarry side and fragmented. Little movement was observed at the back of the block. The block had a crack running directly backwards from the borehole that split the cube in half. No VoD was measured in this cube, but the borehole was expanded over the expected charge length.

The second cube showed much less fragmentation and the throw is directed downwards from an early stage. The fracturing involved two large pieces that rotated outwards. The far piece was held up by two reinforcing rods from the top of the shuttering that had remained undetected a few centimetres below the top of the cube. It is suspected that only about 30% of the borehole detonated completely. It is unclear what happened in the remaining portion though a study of the borehole wall does indicate that some detonation has occurred. There may have been a gap between portions of the product as this cube proved to be very difficult to charge. A VoD of 3033 m/s was measured on average over 0.45 m, with portions recording up to 4359 m/s.

The fracture pattern of the third cube was very similar to that of the first cube. The blast resulted in considerable fragmentation. This cube fragmented into a large quantity of small pieces, which were thrown up to 16 m from the original face. A VoD of 4397 m/s was measured on average over 0.5 m with the first 0.3 m having a VoD of 5110 m/s.

The fracturing of the fourth cube seemed quite similar to the second cube though indications from the borehole expansion are that the whole explosive column fired. The cube broke into a few larger pieces. In this case, a sub-horizontal fracture formed near the base of the charge, being angled slightly upwards towards to the back of the cube. The entire back portion of the cube seems to have been displaced backwards and upwards a few centimetres, probably by sliding along this fracture surface.

The two distinct types of breakage are further confirmed by a study of the face velocities measured

by tracking blocks in the high speed video. The average velocity of the top of the cube 1 was 8.6 m/s and for cube 3 it was 8.5 m/s. The velocity of the same point in cubes 2 and 4 is only 3.4 m/s. There is, however, a difference in the curvature of the face in the early stages of heave. Cubes 1 and 4 showed relatively high velocities at the base of the charge near the middle of the block, but the centre of cube 4 moved faster than the top.

## 7 INSTRUMENTATION RESULTS

There are significant disturbances on the accelerometer traces in cubes 2 and 3 coinciding with detonation. This may be due to electromagnetic interferences, or loose connections due to the cracks in the cast rods. These results are still being analysed and are not discussed further. The 3D geophone arrays successfully recorded good traces in cubes 2 to 4.

The early parts of these traces are shown in Figure 9 for the horizontal geophone that was aligned parallel to the side of the cube. Cubes 2 and 3 also show some disturbances at the start of detonation. The shape of the waveforms is very consistent; however the amplitude and period vary considerably. Preliminary numerical modelling results are used to identify the reasons for the discrepancies.

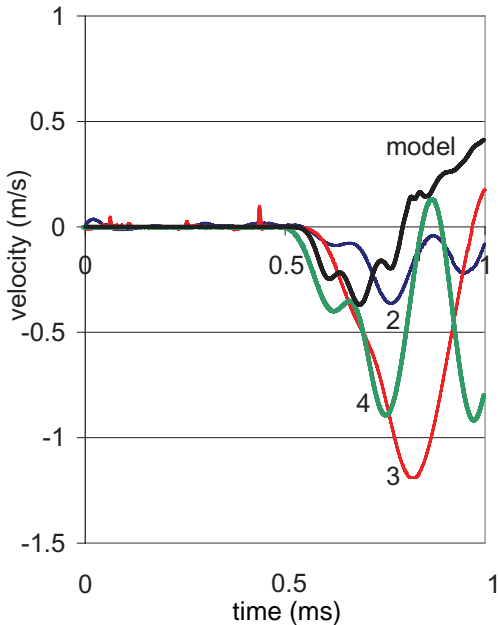


Figure 9. Geophone traces in x-direction measured at the back top corner for the last 3 cubes.

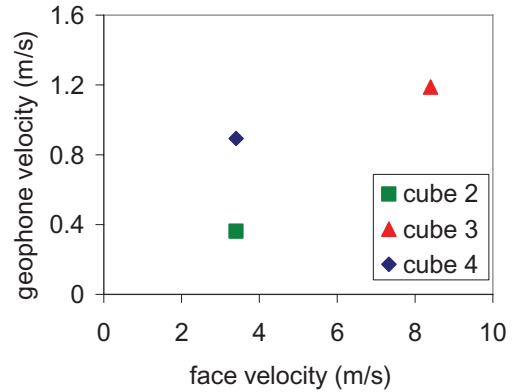


Figure 10. Relationship between face velocity and the peak particle velocity in x-direction measured for the first compressive peak at the geophones.

Also of interest from the data is the relationship between the face velocity and the measured particle velocities within the concrete, as shown in Figure 10. The test with a higher face velocity also showed higher particle velocities. The difference between the results of cube 2 and cube 4 must still be explained, but is probably due to the difference in the quality of the detonation.

## 8 MODELLING OF VELOCITIES

A cube model was developed in version 2 of the HSBM model (Furtney et al. 2009), which uses a lattice method to calculate the particle velocities and determine the blast induced fracture pattern. The numerical methods are explained in detail by Furtney et al. (2009). The cube has a 3 m side length and a lattice spacing of 25 mm. At present, only predefined spacings are available and 25 mm is slightly larger than the aggregate size, but smaller than the borehole diameter. The model uses about 1.4 Gb of memory and take about 20 minutes to run for 1 ms. The concrete is modeled with a density of 2500 kg/m<sup>3</sup>, Young's modulus of 25 GPa, Poisson's ratio of 0.25, compression strength of 45 MPa and tensile strength of 4 MPa, which are the default properties for concrete provided in the user interface. A default small diameter emulsion explosive is used.

The model is shown in Figure 11 and a horizontal slice showing the fracture development is shown in Figure 12. The model confirms the experimental observations that the selected burden is around critical and hence there is limited throw of fragments in the model. It appears that the model produces too much distributed microcracking and

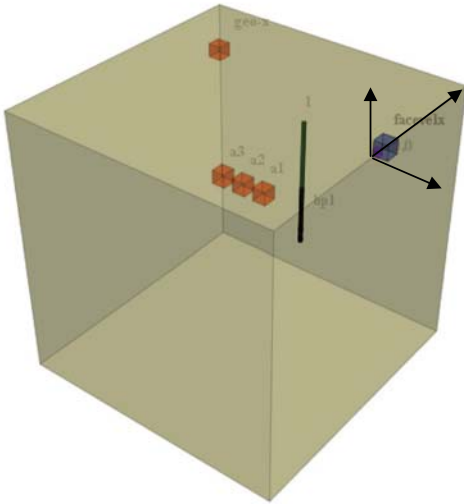


Figure 11. Three dimensional view of the HSBM cube model.

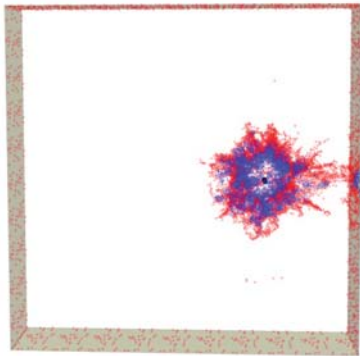


Figure 12. Slice of the HSBM model showing the fracture zone surrounding the borehole and the extending tensile fractures after 1 millisecond of analysis.

insufficient long through-going fractures and this is the subject of current research in the project.

The model prediction of the velocity trace in the x-direction at the geophones is shown in Figure 6 along with the measurements. The shape of the trace is very similar to that of the observations. There is a negative peak in velocity consistent with the arrival of the compression wave, followed by a slight positive movement then a larger negative peak. The slight movement in the positive direction is due to the interaction of the wave reflecting off the back and side of the model 300 mm away with the incoming compressive wave and is not obvious in a model with no free faces. The magnitude of the velocity is at the low side of the observed range,

but the fact that it is within the range of variability of the experimental results justifies the decision to conduct four similar tests. The differences will be addressed as part of future research.

A number of additional model runs were undertaken to investigate the effect of the various parameters that were known to have varied in the experimental procedure. The effect of the compression wave speed is shown in Figure 13. The wave speed was varied by altering the Young's modulus in the measured range and the relevant values are shown in Figure 10. Obviously, as the wave speed increases the wave arrives earlier. Also, the reflected wave arrives earlier and interacts with the incoming compression wave, which is still increasing. In the case of the fastest wave speed this causes only an inflection in the wave trace, whereas the dip in the waveform becomes more obvious at slower wave speeds.

Since a wide range of detonation velocities were measured, it is instructive to evaluate the effect of VoD by overriding the values predicted by Vixen2009 to use a lower reaction completion factor and hence produce less energy at a lower VoD. Figure 14 shows that the slower VoD produces a significantly lower particle velocity and a slower rise time as expected due to the longer time that the explosive is acting over the charge length. This shows why a realistic numerical model is important and that the instantaneous application of the charge often used in models cannot produce correct waveform response.

The VoD traces indicated that the detonated lengths were less than the measured product length in some cubes. The model was used to investigate the influence of having lower charges at the bottom

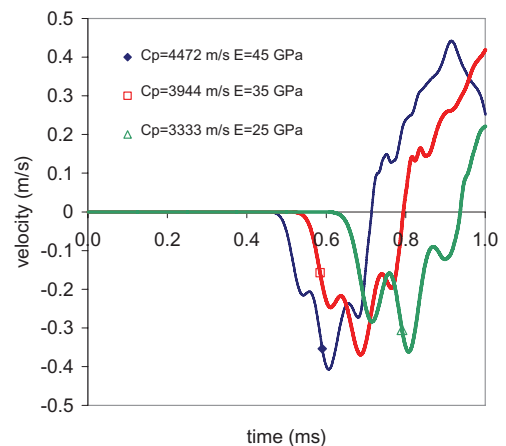


Figure 13. Modelled effect of compression wave speed ( $C_p$ ) for three Young's moduli ( $E$ ) on velocity in x-direction.

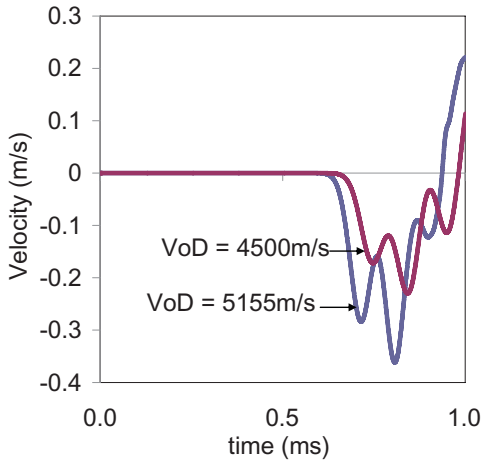


Figure 14. Modelled effect of VoD on velocity in x-direction.

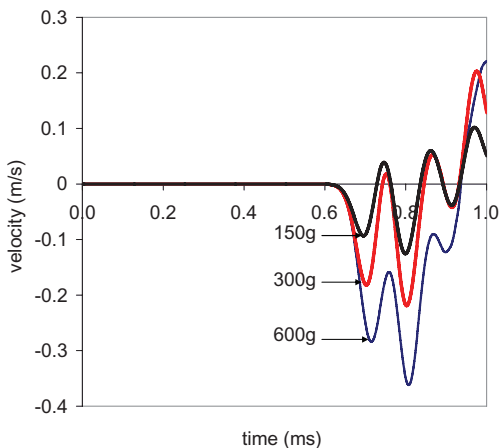


Figure 15. Modelled effect of explosive mass on velocity in x-direction.

of the borehole. Three values of 150 mm, 300 mm and 600 mm were used, being equivalently 150 g, 300 g and 600 g for this diameter and density. The results in Figure 15 indicate that the smallest charge shows the least particle velocity as anticipated, and also has a relatively large rebound after the first peak.

## 9 CONCLUSIONS

Four large scale calibration test blasts have been done for the HSBM project by constructing concrete cubes of 3 m side length to provide a uniform

material for comparison with model results. The amount of explosive (600 g) and borehole diameter (33 mm) were selected to reproduce realistic non-ideal detonation response in the explosive column, cause significant fracturing, but not total destruction so that the situation is suitable for comparison with the numerical models.

Little (1981) notes that “The purpose of an experiment is to answer questions. The truth of this seems so obvious, that it would not be worth emphasizing were it not for the fact that the results of many experiments are interpreted and presented with little or no reference to the questions that were asked in the first place.” In this case, the questions to be asked were essentially:

- Is the experimental data reproduced by the model within the variability of the data?
- Can the model provide us with more information than was known without it?

The answer to the first question must be a qualified yes. Certainly, using default material properties, the model response is found to be similar to that observed, but at the lower end of the measured variability. The cubes were all designed to have the same blast configuration to evaluate the variability of such large scale field tests, which is seldom done due to the high cost and practical difficulties in performing such experiments.

As it turned out this decision was justified as there were differences in the construction; explosive performance; material properties; instrument placement and performance due to the practical difficulties of creating concrete cubes on this scale. These differences have produced a variety of results. Two cubes experienced significant heave and fragmentation whereas the other two broke into large segments that were only displaced slightly. Thus, it appears that the selected burden of 0.8 m is just on critical and this provides another constraint on the modeling.

The answer to the second question is also affirmative and helps in providing insight into the discrepancies between the model with the default properties and the observations that can assist with further research to fine tune the model inputs. Time for modeling the experiments has been limited and so only some brief comparisons with the geophone results are shown. The peak particle velocities from the model are in the same range, but at the lower end of the observed results. The model shows the same waveform shape, but the shape is dependent on the wave speed due to the superposition of reflections from the side of the cube. Modelled waveforms indicate that the period of the waveform increases with charge size and decreases with VoD. The amplitude decreases with charge size and increases with VoD.

We have learnt a significant amount about blasting and the experimental process on this project. In retrospect, the hole diameter of 33 mm is probably too small, as it contains a shocktube, two VoD probes, a trigger wire and still needs space for explosive. The explosive density was too high and was too stiff; a lower density product in a larger hole would probably produce more consistent results. More geophones, situated in regions not expected to move significantly would help to further constrain the model results. The use of tri-axial accelerometers and geophones would be preferable to minimize ambiguity in the interpretation of the data that arises when deciding if a measured peak is the maximum value or a component due to misalignment of a uniaxial sensor.

These experiments have provided significant amounts of information, which will provide validation of the HSBM modeling results. Hopefully, both the test data and the learning from performing these experiments will be of use to the broader blasting community in future.

## ACKNOWLEDGEMENTS

The authors wish to gratefully acknowledge the sponsors of the HSBM project who are African Explosives Limited (AEL), De Beers, Debswana Diamond Company, Anglo American, Codelco IM2, LKAB, Sandvik Mining and Construction, Dyno Nobel Asia Pacific and Rio Tinto. In addition the authors wish to thank the Executive Steering Committee (ESC) members for allowing the publication of this paper. The team would like to acknowledge the provision of some sensors from De Beers and explosives from AEL as well as people from De Beers and AEL who assisted. In particular we would like to thank Dave Tyler and Charlene Hugo for manufacturing the explosive; Andrew Mbembe, Andre Pienaar and Andries Botha for their assistance. We also thank Luis Valentim of TLC for data collection. We thank the reviewers for helpful comments.

## REFERENCES

AEL. 2000. *Explosive engineers course*. Johannesburg: African Explosives Limited.  
 Bergmann, O.R., Riggle, J.W. & Wu, F.C. 1973. Model rock blasting effect of explosives properties and other variables on blasting results. *Int. J. Rock. Mech. Min. Sci. & Geomech. Abst.* 10: 585–612.  
 Braithwaite, M., Sharpe, G.J. & Chitombo, G.P. 2009. Simulation of real detonations as an energy source term for

the Hybrid Stress Blasting Model. In J.A. Sanchidrián (ed.), *Proc. 9th Int. Symp. on Rock Fragmentation by Blasting—FRAGBLAST 9*, Granada, Spain, 13–17 September. Rotterdam: Balkema.  
 Cundall, P.A. & Detournay, C. 2008. Modeling shock and detonation waves with FLAC. *Proc. 1st Int. FLAC/DEM Symp. on Numerical Modeling*, 25–27 August, Minneapolis. Itasca.  
 Cunningham, C., Braithwaite, M. & Parker, I. 2006. Vixen Detonation Codes: Energy Input for the HSBM. *Proc. 8th Int. Symp. on Rock Fragmentation by Blasting—FRAGBLAST 8*. Santiago, Chile, 7–11 May. Santiago: Editec, pp. 169–174.  
 Dick, R.D., Fourney, W.L., Wang, X.J. & Young, C. 1993. Results from instrumented small scale model tests. In H.P. Rossmanith (ed.), *Proc. 4th Int. Symp. on Rock Fragmentation by Blasting—FRAGBLAST 4*, Vienna, 5–8 July, pp. 47–54. Rotterdam: Balkema.  
 Esen, S., Onederra, I. & Bilgin, H.A. 2003. Modelling the size of the crushed zone around a blasthole. *Int. J. Rock Mech. & Min. Sci.* 40: 485–495.  
 Furtney J., Cundall, P.A. & Chitombo, G. 2009. Developments in numerical modeling of blast induced rock fragmentation: Updates from the HSBM project. In J.A. Sanchidrián (ed.), *Proc. 9th Int. Symp. on Rock Fragmentation by Blasting—FRAGBLAST 9*, Granada, Spain, 13–17 September. Rotterdam: Balkema.  
 Katsabanis, P.D., Tawadrous, A., Braun, C. & Kennedy, C. 2006. Timing effects on fragmentation. *Proc. 32nd Annual Conf. on Explosives and Blasting Technique*, Dallas, 29 January–February 1. Cleveland, OH: International Society of Explosives Engineers.  
 Kristiansen, J., Kure, K., Vestre, J. & Bergqvist, I. 1990. An investigation of heave and fragmentation related to explosive properties. *Proc. 3rd Int. Symp. on Rock Fragmentation by Blasting*, Brisbane, QLD, 26–31 August. Carlton, VIC, Australia: Australasian Institute of Mining and Metallurgy.  
 Little, T.M. 1981. Interpretation and presentation of results. *Hortscience* 16: 637–640. at <http://www.indiana.edu/~stigtsts/quototr.html>  
 Ouchterlony, F., Nie, S., Nyberg, U. & Deng, J. 1996. Monitoring of large open cut rounds by VOD, PPV and gas pressure measurements. In B. Mohanty (ed.), *Proc. 5th Int. Symp. on Rock Fragmentation by Blasting—Fragblast 5*, Montreal, Canada, 25–29 August. Rotterdam: Balkema, pp. 167–178.  
 Potyondy, D.O. & Cundall, P.A. 2004. A bonded-particle model for rock. *Int. J. Rock Mech. & Min. Sci.* 41(8): 1329–1364.  
 Ruest, M., Cundall, P., Guest, A. & Chitombo, G. 2006. Developments using the particle flow code to simulate rock fragmentation by condensed phase explosives. *Proc. 8th Int. Symp. on Rock Fragmentation by Blasting—FRAGBLAST 8*. Santiago, Chile, 7–11 May. Santiago: Editec, pp. 140–151.  
 Stagg, M.S. & Rholl, S.A. 1987. Effects of accurate delays on fragmentation for single-row blasting in a 22 ft bench. *Proc. 2nd Int. Symp. on Rock Fragmentation by Blasting*, Keystone, CO, 23–26 August, pp. 210–230.